Journal of Applied Polymer Science

Effect of processing conditions on the dispersion of carbon nanotubes in polyacrylonitrile solutions

Xuejia Yan,[1*] Hongming Dong,[1†] Yaodong Liu,[1] Bradley A. Newcomb,[1] Han Gi Chae,[1#] Satish Kumar,[1] Zhiwei Xiao,[2] Tao Liu[2]

School of Materials Science and Engineering, Georgia Institute of Technology, Atlanta, Georgia 30332
High-Performance Materials Institute, Florida State University, Tallahassee, Florida 32310
*Present address: Standridge Color Corporation, 1196 E Hightower Trail, Social Circle, GA, 30025, USA
†Present address: The Boeing Company, P.O.Box 3707, MC 06-FW, Seattle WA, 98124, USA
#Present address: School of Materials Science and Engineering, Ulsan National Institute of Science and Technology, Ulsan, 689-798, South Korea
Correspondence to: S. Kumar (E-mail: Satish.kumar@mse.gatech.edu)

ABSTRACT: As a result of van der Waal's interactions, carbon nanotubes (CNTs) tend to assemble into bundle/rope structures. It is essential to de-bundle and exfoliate CNTs in polymer solutions in order to utilize their reinforcement potential as far as possible. In this study, a variety of different processing conditions were used to prepare polyacrylonitrile/CNTs composite solutions. The CNT bundle diameter, length, and macro-scale dispersion homogeneity in those solutions were compared. It was observed that the CNT type, solvent type, and polymer concentration were important factors to determine the CNT bundle sizes in the solutions. The results are expected to be beneficial to obtain well-dispersed polymer/CNT nanocomposites. © 2015 Wiley Periodicals, Inc. J. Appl. Polym. Sci. **2015**, *132*, 42177.

KEYWORDS: composites; graphene and fullerenes; nanotubes; properties and characterization

Received 16 December 2014; accepted 5 March 2015
DOI: 10.1002/app.42177

INTRODUCTION

Carbon nanotubes (CNTs) exhibit exceptional mechanical properties, and are often considered as an ideal material for making high-performance CNT fibers,[1–5] CNT-reinforced polymeric fibers,[6–9] and films.[10,11] Particularly, the high aspect ratios of CNTs make them suitable to reinforce polymer fibers. Polyacrylonitrile (PAN) is the most important precursor for fabricating high tensile and compressive strength carbon fibers.[12–15] With the addition of only 1 wt % CNTs in gel-spun PAN precursor fibers, our group has previously demonstrated that both CNT-reinforced precursor fibers and the resultant carbon fibers possessed significantly improved mechanical properties.[16–18] The templating effect of CNTs for polymer crystallization and orientation, and for graphitic structure development was ascribed to this important finding.

The agglomeration of CNTs is the major challenge for obtaining a high-quality PAN/CNTs solution.[19] The formation of CNT bundles prevents the utilization of their maximum potential to achieve excellent reinforcement for composite materials. In order to make high-performance composite carbon fibers, homogeneously dispersed CNTs in the composite solutions consisting of small CNT bundles or exfoliated CNTs are highly desired. With ultra-sonication as the most frequent dispersion technique, significant efforts have been made to reduce CNT bundle diameter and exfoliate CNT bundles into individual tubes.[20–23] In this article, we focus on the preparation methods of PAN/CNTs composite solutions[24,25] under various processing conditions to elucidate their effect on the CNT dispersion quality, which is critical to produce high-quality PAN/CNT precursor fibers for producing high strength and modulus carbon fibers. The CNT bundle sizes were characterized by combining a preparative ultracentrifuge method (PUM) and dynamic light scattering (DLS).[26,27]

EXPERIMENTAL

PAN polymers with different molecular weights were obtained from Japan Exlan Co., and were dried under vacuum at 70°C overnight before use. Few wall CNT (FWNT) XO021UA (aspect ratio ~1320, average diameter ~3 nm), XO122UA (aspect ratio ~1050, average diameter ~3 nm), and XOC231UA (aspect ratio ~2820, average diameter ~2.7 nm) were obtained from Continental Carbon Technologies. Single wall CNT (SWNT) HiPCO SPO300 (aspect ratio 470–500, diameter 1–2 nm)[28] was obtained from CNI and were used as received. Aspect ratio of

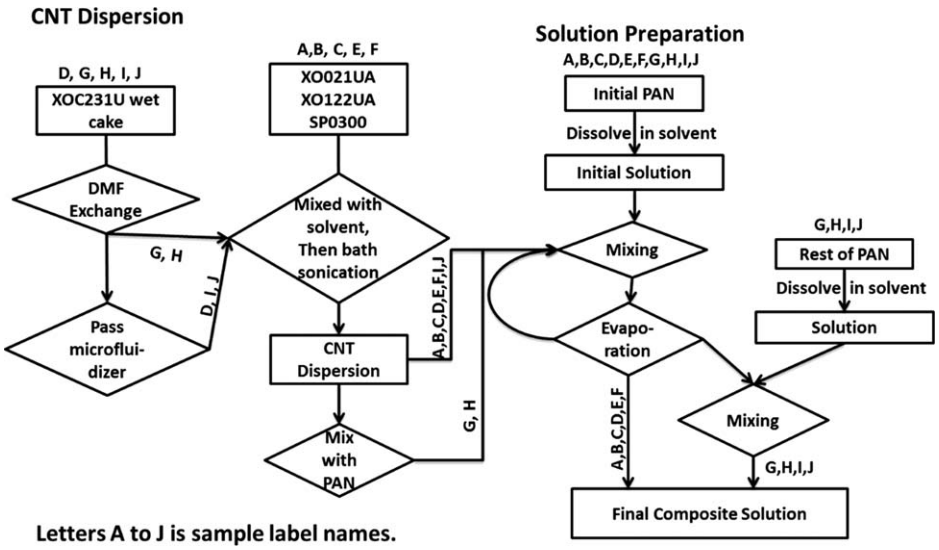

Figure 1. Processing flow of composite solutions.

CNT was measured by an extensional viscosity method[29] according to the theory of Shaqfeh and Fredrickson.[30] CNTs XO021UA and XO122UA were received in powder form and were directly used after vacuum drying at 100°C for 1 day. CNT XOC231U was received in wet form containing >97 wt % of water. Before use for composite solution preparation, the water in XOC231U CNT was exchanged first with an organic solvent using the following procedure:

1. Ten grams XOC231U wet cake was mixed with ~400 mL solvent (DMF or DMAc), then bath sonication (Branson 8510 ultrasonic cleaner, 40 kHz, 320 watt output) for 1 h.
2. Water and solvent mixture were removed by vacuum distillation from the mixture of solvent/water/CNT until the volume reduced to about 160 mL.
3. Repeated steps 1 and 2 for a total of four times.
4. Diluted CNT slurry to 0.6 g/L by adding extra solvent, and then kept stirring continuously using a magnetic stirrer bar.

PAN/CNT composite solutions were prepared according to the procedure described elsewhere.[31] Figure 1 shows the process flow-chart and Table I lists the detailed processing conditions for preparing 10 different PAN/CNT composite solutions (A–J). CNT (XO021UA, XO122UA and SPO300) powders were mixed with proper amount of solvent. For CNT XOC231U, water/solvent exchange was conducted to obtain CNT/solvent slurries. For XOC231U containing solutions D, I, and J, the above CNT slurries pass through a micro-fluidizer (Microfluidics, M-110P) to further de-bundle CNTs. All the slurries, 1 g/L, were constantly stirred by a magnetic stirrer before use for bath-sonication. For CNT dispersion preparation, these slurries were diluted with proper amount of solvent to a desired concentration, typically 4–30 mg/L, and then were bath-sonicated for 24 h to disperse CNTs. For CNT dispersions obtained after bath-sonication, dispersions A, B, C, D, E, F, I, and J, were directly transferred into the initial PAN solutions for further distillation process to increase CNT concentration in the solution. While dispersions, G and H, were first mixed with an appropriate amount of neat PAN solution (1 g/dL) to stabilize the CNT dispersion, and then mixed with the initial PAN solutions. The CNT dispersions were transferred into the glass reactor using vacuum suction through a Teflon tube. During distillation/evaporation, excess solvent was removed under vacuum to increase CNT concentration and concentrate the PAN/CNT solution until the desired concentrations were achieved. For PAN solutions, A, B, C, D, E, and F, all PAN was dissolved in the initial solution prior to the addition of CNT dispersions, and the final composite solutions were obtained right after evaporation. While solutions, G, H, I, and J, part of the PAN was dissolved in the initial solution for preparing composite solution portions. The rest of PAN was dissolved separately, and both solutions were mixed together to obtain the final composite solutions.

Macroscopic CNT dispersion of composite solutions was assessed on a Leica optical microscope (DM 2500P, Leica). High-resolution transmission electron microscopy (TEM) was carried out on a high-resolution TEM (JEOL JEM-ARM200F) operated at 80 keV. To prepare the TEM sample, the PAN composite solutions were diluted to a concentration of 0.1 g/dL by adding extra solvent, and then magnetically stirred for 8 h at 70°C. The diluted solutions were dropped onto TEM copper grids (Lacey Formvar/Carbon, 300 meshes). The excess solvent was removed by a filter paper from the back side of the TEM grid. The diluted solutions were also subjected to PUM characterization with an Optima™ MAX-XP ultracentrifuge instrument (30° fixed angle rotor, Beckman Coulter) to determine the sedimentation coefficient of CNTs. The diffusion coefficient of CNTs in the diluted solution was measured by DLS technique carried out at 25°C with Delsa Nano C (Beckman Coulter) at a fixed scattering angle of 166° with a laser of 658 nm wavelength.

RESULTS AND DISCUSSION

The diffusion coefficient (D) of the CNT bundles in the diluted composite solutions is related to the bundle size. Larger diffusion coefficient indicates a smaller CNT bundle size. Similarly,

Table I. Detailed Processing Conditions for PAN/CNT Composite Solutions

Sample label		A	B	C	D	E
Materials	PAN type	$Homo_{250K}$	$Homo_{250K}$	$Homo_{250K}$	$Homo_{250K}$	MAA_{240K}
	Solvent type	DMF	DMF	DMF	DMF	DMAc
	CNT type	XO021UA	XO122UA	SP0300	XOC231U	XO122UA
CNT slurry	Solvent exchange	-	-	-	DMF	-
	Homogenizing	-	-	-	30 min	-
	Micro-fludizing	-	-	-	10 cyl	-
CNT dispersion	Bath sonication	30 mg/L, 24 h	30mg/L, 24 h	30 mg/L, 24 h	10 mg/L, 24 h	30 mg/L, 24 h
	$Ratio^{Af\ Sonic}_{PAN/CNT}$	-	-	-	-	-
Composite solution	$PAN_{Initial}$/PAN	100%	100%	100%	100%	100%
	PAN_{Final}/PAN	0%	0%	0%	0%	0%
	$Conc._{PAN}$ (g/dL)	15	15	17	17	15
	CNT/PAN	1%	1%	1%	1%	1%

Sample label		F	G	H	I	J
Materials	PAN type	$Homo_{250K}$	MAA_{513K}	MAA_{513K}	MAA_{513K}	MAA_{513K}
	Solvent type	DMAc	DMF	DMAc	DMF	DMF
	CNT type	XO122UA	XOC231U	XOC231U	XOC231U	XOC231U
CNT slurry	Solvent exchange	-	DMF	DMF	DMF	DMF
	Homogenizing	-	-	-	-	-
	Micro-fludizing	-	-	-	20 cyl	20 cyl
CNT dispersion	Bath sonication	30 mg/L, 24 h	4 mg/L, 24 h	4 mg/L, 24 h	6 mg/L, 24 h	6 mg/L, 24 h
	$Ratio^{Af\ Sonic}_{PAN/CNT}$	-	40	120	-	-
Composite solution	$PAN_{Initial}$/PAN	100%	0%	20%	25%	40%
	PAN_{Final}/PAN	0%	80%	50%	75%	60%
	$Conc._{PAN}$ (g/dL)	15	10.5	10.6	12	10.6
	CNT/PAN	1%	0.5%	0.25%	0.45%	0.5%

PAN type: $Homo_{250K}$ is a homopolymer PAN with a viscosity molecular weight of 2.50×10^5 g/mol; MAA_{240K} is a copolymer PAN-co-MAA (4%) with a viscosity molecular weight of 2.40×10^5 g/mol; MAA_{513K} is a copolymer PAN-co-MAA (4%) with a viscosity molecular weight of 5.13×10^5 g/mol. $Ratio^{Af\ Sonic}_{PAN/CNT}$: the weight ratio of the added PAN over CNTs after bath sonication. $PAN_{Initial}$/PAN: weight fraction of PAN that was dissolved in solvent in the beginning; PAN_{Final}/PAN: weight fraction of the rest of PAN that was dissolved separately for final mixing; $Conc._{PAN}$ (g/dL): PAN concentration in the final composite solution.

the sedimentation coefficient, which is defined as the ratio of a particle's sedimentation velocity to the acceleration that is applied to it, of the CNT bundles in the diluted composite solutions provides another type of measurement of the CNT bundle size. The larger the sedimentation coefficient, the faster is the sedimentation velocity, and the larger is the particle size. With the sedimentation coefficient determined by PUM and the diffusion coefficient measured by DLS, we have the s/D ratio (cm^2/s^2) that is proportional to the mass of CNT particles as indicated by the Svedberg equation provided below:

$$\frac{s}{D}=\frac{m(1-v\rho_0)}{kT} \tag{1}$$

where m is the mass of the bundle; v is the partial specific volume of the bundle; ρ_0 is the density of solvent; k is Boltzmann constant; and T is absolute temperature. As suggested by eq. (1), s/D is only a function of bundle mass and does not depend upon the size/shape of the CNT bundles. By considering the rod-like nature of CNTs, one can estimate the average length and diameter of CNT bundles in the composite solutions with the following equations:[27]

$$\hat{s}=s\frac{12\eta}{(v^{-1}-\rho_0)}=d^2[\ln(L/d)+2\ln 2-1] \tag{2}$$

$$\hat{D}=D\frac{3\pi\eta}{kT}=\frac{1}{L}[\ln(L/d)+2\ln 2-1] \tag{3}$$

where $\hat{s}$ and $\hat{D}$ are the rescaled sedimentation and diffusion coefficients, respectively, η is the viscosity of the solution, L is the length of the CNT bundle, and d is the diameter of CNT bundle. As suggested by eq. (2), the sedimentation coefficient varies more sensitively with the CNT bundle diameter but not length, since it has a power of two dependence on the bundle diameter and a logarithmic dependence on the bundle length. Similar arguments applied to eq. (3), where the diffusion coefficient of the CNT bundles in the composite solutions is more sensitive to the variations of CNT bundle length.

Table II. CNT Bundle Sizes as Calculated from DLS and PUM Methods

Sample	s ($\times 10^{-11}$ s)	D ($\times 10^{-9}$cm^2/s)	s/D ($\times 10^{-3}$ s^2/cm^2)	Length (μm)	Diameter (nm)	Aspect ratio
A	4.26	5.22	8.2	4.9 ± 0.3	13.2 ± 1.5	371 ± 64
B	4.05	4.89	8.3	5.3 ± 0.3	12.8 ± 1.4	414 ± 68
C	1.48	8.06	1.8	3.2 ± 0.2	7.8 ± 0.9	410 ± 73
D	1.29	2.48	52.2	10.5 ± 0.7	22.9 ± 2.6	458 ± 86
E	9.56	3.37	28.4	7.7 ± 0.5	19.8 ± 2.3	389 ± 70
F	9.37	3.60	26.0	7.1 ± 0.5	19.7 ± 2.2	360 ± 65

It is noted that both the sedimentation and dynamic light scatting experiments were performed in diluted PAN/CNT dispersions with a polymer concentration of 0.1 g/dL. At such a low polymer concentration, the density as well as the refractive index of the polymer solution expects to be the same as those of the neat solvent. In addition, because of the much larger size of CNT bundles as compared to PAN molecules, the scattering power of CNT far exceeds that of PAN polymer. As a consequence, this renders the scattering intensity out of the PAN/CNT/Solvent ternary system mostly contributed by CNTs as evidenced by our previous work.[32] For the above mentioned reasons, the influence of free polymer on the PUM and DLS measurements to determine CNT bundle length and diameter is minimal. However, the presence of polymer can indeed increase the solution viscosity and therefore reduce the sedimentation and diffusion coefficient of CNT bundles when compared with the CNT/solvent neat dispersions. With regard to the calculation of L and d, this effect has been taken into account by using the viscosity of polymer solutions to calculate the rescaled sedimentation and diffusion coefficients. At 0.1 g/dL, the relative viscosity η_B/η_s of the polymer solution prepared with PAN with a viscosity average molecular weight of 250,000 and 500,000 g/mol was 1.432 and 1.683, respectively, according to our previous work.[32]

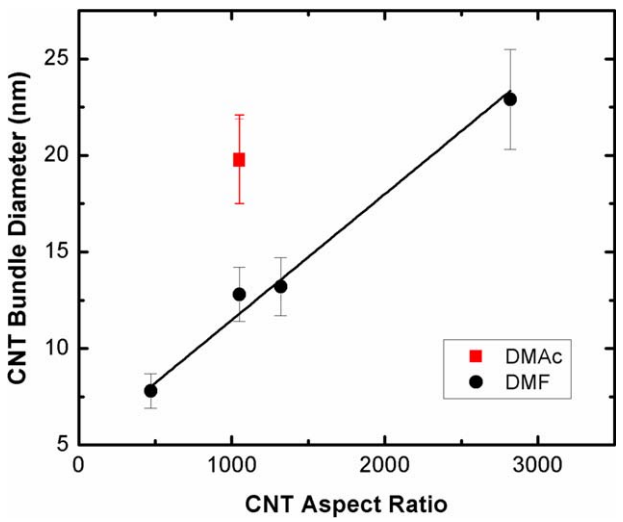

Figure 2. Measured CNT bundle diameters versus the aspect ratios of as-received CNT. [Color figure can be viewed in the online issue, which is available at wileyonlinelibrary.com.]

Effect of PAN, CNTs, and Solvent Types on CNT Bundle Sizes

CNT bundle length and diameter were calculated based upon eqs. (1–3). Table II lists the results for the composite solutions (from A to F) prepared under the processing conditions given in Table I. It should be noted that XOC231U could not be well dispersed in DMF at 30 mg/L after 24 h bath sonication, and visible agglomerations were observed. For this reason, the CNT dispersion concentration of Sample D was lowered to 10 mg/L. Samples A, B, C, and D were prepared under the same processing conditions while altering the CNT types. CNT bundle diameter as determined from the equations above, exhibits a linear dependence on the aspect ratios of as-received CNTs as shown in Figure 2. For composite solution D containing XOC231U tubes which have the highest aspect ratio, the CNT bundle size was the largest among all solutions. Above results suggest that the de-bundling and exfoliation of CNTs become much more difficult when the CNT aspect ratio is higher.

The composite solution E and F were prepared under same processing conditions, with the exception of the type of PAN polymers. One is homopolymer (F) and the other is copolymer (E). Both polymers contain similar viscosity average molecular weights (M_v) with the difference being the 4 mol % addition of methacrylic acid (MAA) copolymer. It was observed that CNTs in solutions E and F have statistically identical bundle diameters, which suggests that the type of polymers, either PAN-co-MAA or Homo-PAN, had negligible effect on the CNT bundle diameter. The aspect ratios of CNT bundles in polymer solution are ~400 which is smaller and also independent on the aspect ratio of as-received CNTs.

The composite solutions B and F were processed under same processing conditions, except for the solvent used (DMF and DMAc, respectively). Solution F showed a 34% larger bundle diameter than solution B, which suggests that DMF has a better interaction with CNTs as compared to DMAc. The increased interaction between CNT and DMF results in a reduced bundle length and diameter, and it allows for higher concentrations of CNTs dispersed in DMF, while maintaining a bundle size comparable with that in DMAc/CNT dispersions.

CNT Bundle Size Changes During Condensing and Mixing

The composite solutions G and H were obtained by mixing the concentrated PAN/CNT solutions with a separately prepared PAN solution as noted in the experimental section. The processing flow of G and H is shown in Figure 3. The rationale for doing this is to minimize the polymer degradation during

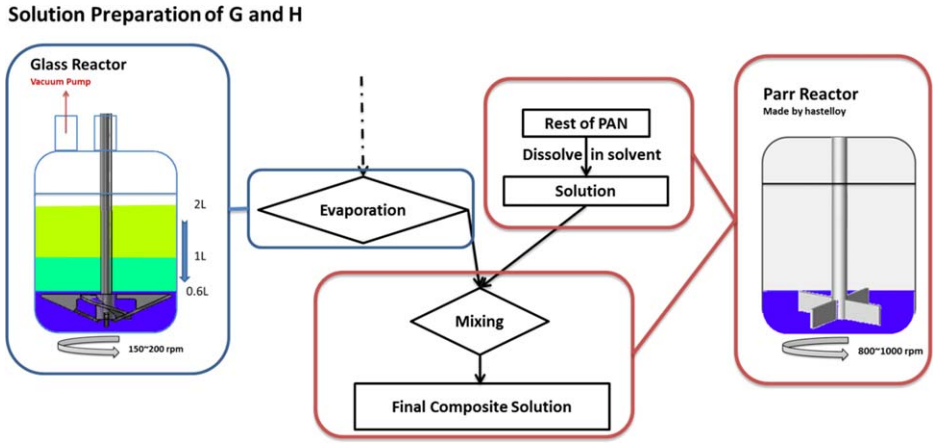

Figure 3. Solution mixing flow of G and H, and schematic descriptions of glass and Parr reactors. [Color figure can be viewed in the online issue, which is available at wileyonlinelibrary.com.]

solvent distillation process which typically takes 5–7 days. CNT bundle length and diameter analysis results are shown in Table III. After all CNTs were added into the initial PAN solution, three samples were collected at the point when the remaining solution volume (as the distillation progressed) was 2 L, 1 L, and 600 mL (see scheme of glass reactor in Figure 3), and they were denoted as G_2L, G_1L, and G_Glass, respectively. The remaining PAN was dissolved separately in the Parr reactor, and then mixed with the PAN/CNT solution that was obtained by evaporation to form the final solutions. It is noted that G_Glass and H_Glass samples were collected before mixing in the Parr reactor, and G_Parr and H_Parr were collected after high shear mixing in Parr reactor. The schematics of the glass and Parr reactors are also shown in Figure 3. Comparing the glass reactor and Parr reactor, the Parr reactor can provide ~three times higher shear force, which will promote the homogeneous dispersion of CNTs in PAN solutions.

The sedimentation coefficient of CNT bundles did not change much when solution G was concentrated from 2 L (G_2L) to 1 L (G_1L), but reduced significantly when the solution volume further decreased from 1 L (G_1L) to 550 mL (G_Glass) in the glass reactor, as well as after shearing with fresh PAN solution in Parr reactor (G_Parr). In accordance with this observation, the *s/D* ratio, which is proportional to the mass of the CNT bundles, shows a similar trend. During the concentration process, the solvent evaporation resulted in an increased polymer concentration, and therefore an increased solution viscosity. As a consequence, the shear stress would increase even though the composite solution was kept stirring at a constant speed (constant shear rate), since the shear stress is proportional to both shear rate and viscosity. It appears that the increase in shear stress was significant when the solution volume was reduced below 1 L, which facilitated the de-bundling of CNTs. After mixing the G_Glass and H_Glass composite solutions with their corresponding fresh PAN solutions in the Parr reactor, the solution was further sheared in the Parr reactor at a much higher stirring speed than that in the glass reactor. The higher shear stress caused by higher shear rate was favorable for further de-bundling of CNTs. However, it can be noted that the calculated bundle length of G_Parr as compared to G_2L and G_1L (Table III) increased slightly in this process, which appears to be contradictory. The possible reason is that the bundle diameter and length are calculated from a model which assumes a rigid rod geometry for the CNTs. XOC231U CNTs are much longer than

Table III. CNT Bundle Sizes in Composite Solutions During Condensing and Mixing

Sample	s ($\times 10^{-11}$ s)	D ($\times 10^{-9}$ cm^2/s)	s/D ($\times 10^{-3}$ s^2/cm^2)	Length (μm)	Diameter (nm)
G_2L	14.7	2.64	55.6	7.5 ± 0.5	27.9 ± 3.2
G_1L	14.1	2.48	57.0	8.2 ± 0.5	27.1 ± 2.9
G_Glass	5.31	2.00	26.6	12.0 ± 0.8	15.5 ± 1.7
G_Parr	3.04	2.32	13.1	10.0 ± 0.6	11.6 ± 1.3
H_Glass	9.80	2.45	40.0	6.9 ± 0.5	24.8 ± 2.8
H_Parr	4.59	2.60	17.6	4.4 ± 0.3	20.6 ± 2.4

G_2L: Composite solution of sample G prepared in glass reactor, solution was undergoing evaporation and the residual volume of solution was 2L. PAN: 2.7 g/dL, CNT/PAN=2.5%. G_1L: Composite solution of sample G prepared in glass reactor, solution was undergoing evaporation and the residual volume of solution was 1L. PAN: 5.5 g/dL, CNT/PAN=2.5%. G_Glass: Composite solution of sample G prepared in glass reactor, the evaporation was completed, and the residual volume of solution was 0.55 L. PAN: 9.5 g/dL, CNT/PAN=2.5%. G_Parr: Sample G final solution after mixing in Parr reactor with the rest of PAN with a better shearing than in glass reactor. PAN: 10.5 g/dL, CNT/PAN=0.5%. H_Glass: Composite solution of sample H prepared in glass reactor. PAN: 10.6 g/dL, CNT/PAN: 0.5%. H_Parr: Sample H final solution after mixing in Parr reactor with the rest of PAN. PAN: 10.6 g/dL, CNT/PAN: 0.25%.

Table IV. CNT Bundle Sizes from DLS and PUM in Composite Solution Samples I and J

Sample	Initial PAN percentage	s ($\times 10^{-11}$ s)	D ($\times 10^{-9}$cm^2/s)	s/D ($\times 10^{-3}$)	Length (μm)	Diameter (nm)
I	25%	12.2	2.2	55.8	9.7 ± 0.6	24.7 ± 2.6
J	40%	6.4	3.6	17.8	5.7 ± 0.4	18.2 ± 2.1

other CNTs used in this study, and are more flexible because of their high aspect ratio. In this case, the model may have limitation to predict the bundle lengths. The average bundle diameter of sample H was larger than that of sample G, which could be attributed to the different solvents used in samples H (DMAc) and G (DMF), as discussed in the previous section.

Effect of Initial PAN Concentration on CNT Bundle Sizes

Solutions I and J were prepared under the same processing conditions with the exception of different initial PAN concentrations. The measured average CNT bundle length and diameter are shown in Table IV. Solution J had a significantly smaller CNT bundle diameter, which indicates that the higher initial PAN concentration reduces CNT bundle sizes in the composite solutions. The reduction of CNT bundle size may be because of the following reasons: (1) higher initial PAN concentration allowed more polymer chains to stabilize dispersed CNTs; (2) higher initial viscosity is favorable to slow down CNT aggregation during solution preparation as well as de-bundle CNTs. Figure 4 provides the image analysis results of optical images of composite solutions, I and J. The full width at half maximum (FWHM) of the normalized image histogram indicates the CNT concentration fluctuation in composite solutions. A smaller FWHM value indicates a smaller concentration fluctuation of CNTs in the composite solution, and suggests a more uniform dispersion of CNTs. It can be observed that composite solution J which used more initial PAN showed better homogeneity of CNT dispersed than composite solution I.

Microscope Study of Composite Solutions with Different CNT Types

Figure 5(a) is a TEM image of solution G. The measured average diameter of the PAN/XOC231U CNT bundles [Figure 5(a)] was 13.0 nm, and was much smaller than the bundle diameter

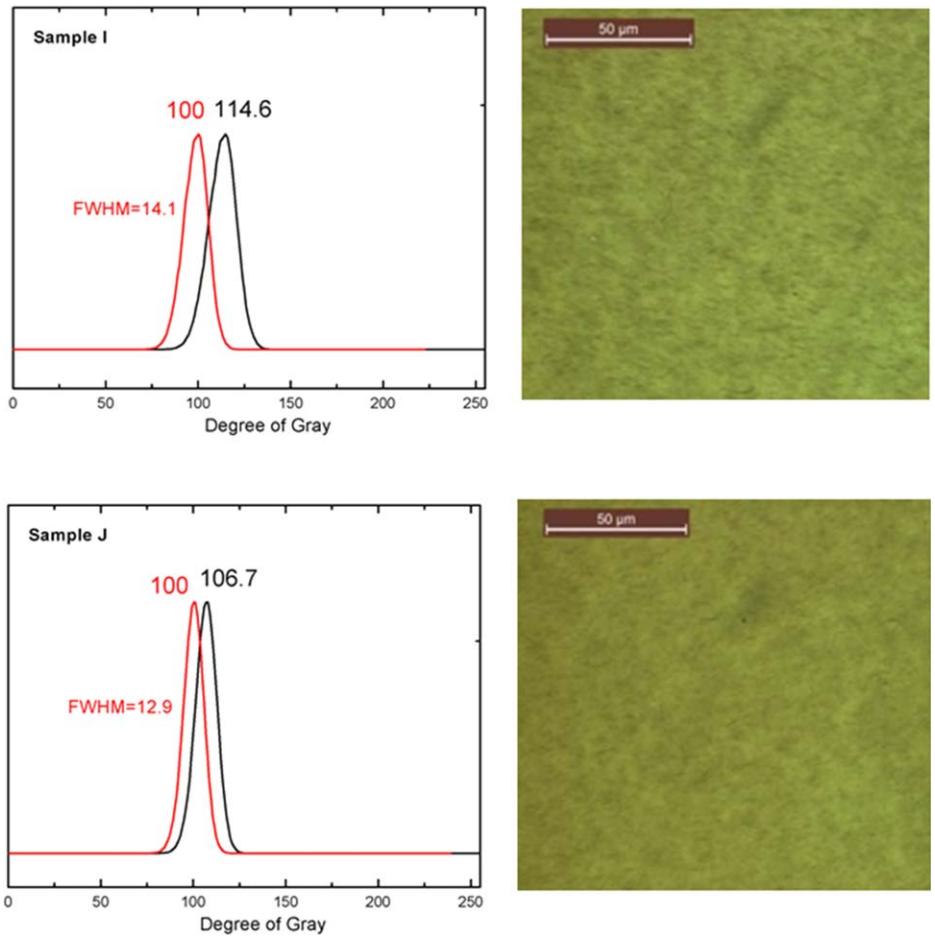

Figure 4. Optical image analysis of samples I and J composite solutions. Black curves are image histograms, and red curves are normalized histograms. [Color figure can be viewed in the online issue, which is available at wileyonlinelibrary.com.]

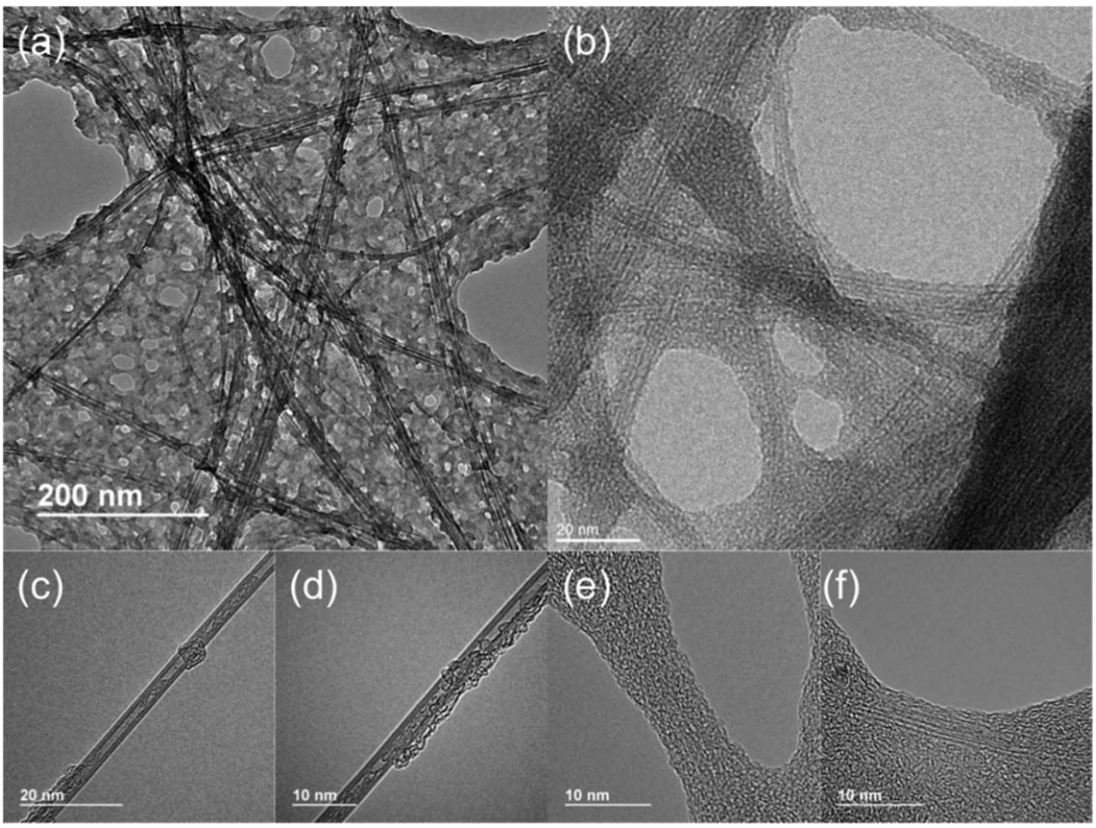

Figure 5. High-resolution TEM (80 kV) images of (a) PAN/XOC231U composite solutions (sample G) and (b) dissolved PAN/XOC231U fibers. High-resolution TEM images of (c) and (d) are sample G solution, and (e) and (f) are sample C solution (PAN/SPO300).

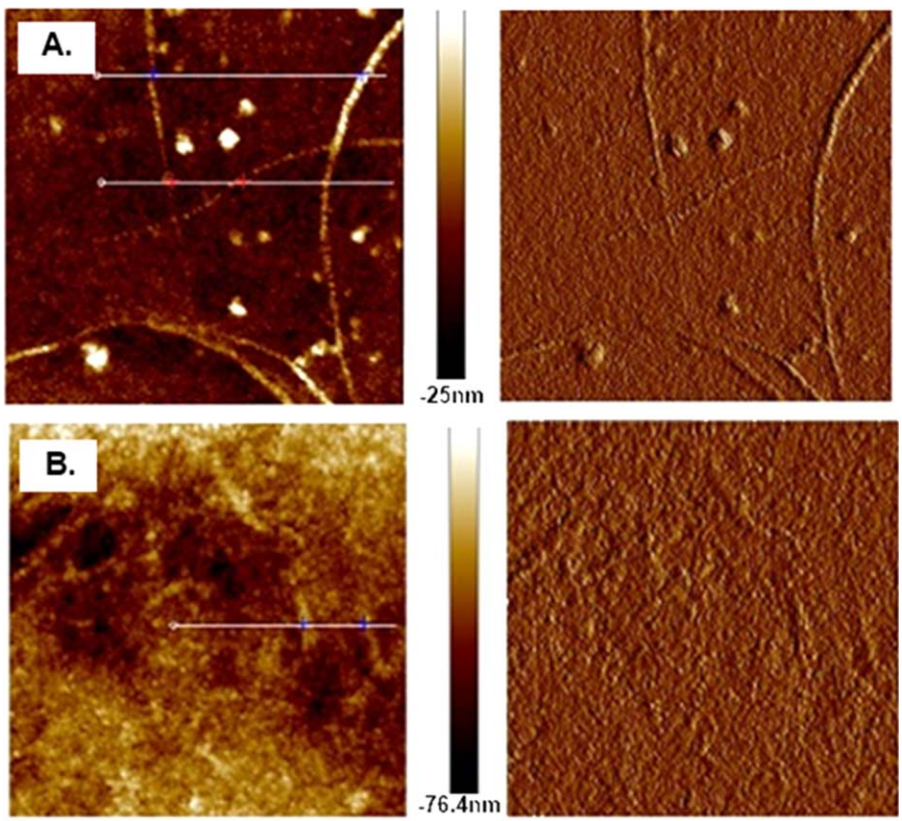

Figure 6. Dual height and phase AFM images of (A) PAN/XOC231U composite solutions (sample G) and (B) PAN/SPO300 composite solutions (sample C). Image scale: 5 × 5 μm. [Color figure can be viewed in the online issue, which is available at wileyonlinelibrary.com.]

from PUM and DLS results (27.9 ± 3.2 nm). From the TEM image, it can be observed that the PAN polymer was adhered to the CNTs which may increase the CNT bundle mass as determined by PUM and DLS. The larger value from PUM and DLS data may indicate that the CNT bundles in the composite solution were wrapped with PAN molecules. Fiber spun from solution G was then dissolved in DMF at near boiling temperature and observed by high-resolution TEM as shown in Figure 5(b). From Figure 5(b), the average diameter of CNT bundles was measured to be about 6.8 nm. Although the bundle diameter from TEM shows a localized set of information and may not represent the average value of the entire sample, the smaller diameter of CNTs in the dissolved precursor fiber compared to that in composite solution may indicate that the CNTs can be further de-bundled during the fiber spinning and drawing stages because of polymer chain stretching. Similar de-bundling has been observed in PAN/SWNT fibers, where de-bundling occurs during the fiber manufacturing process.[25,33] Individual XOC231U tubes could also be observed in the PAN/XOC231U composite solution [Figure 5(c,d)]. Polymer chains are loosely aligned along the CNT surface that can be aligned and crystallized during fiber spinning and drawing. Aligned and crystallized PAN along the CNT surface is advantageous for graphitic template effect in the composite carbon fiber. The PAN/SPO300 composite solution (solution C) showed CNTs and CNT bundles coated in PAN as shown in Figure 5(e,f).

AFM image of composite solutions G and solution C are shown in Figure 6. Compared to PAN/XOC231U composite solution, CNTs in the PAN/SPO300 composite solution were hard to be observed, which can likely be attributed to the smaller bundle size in Solution C as well as to the thick PAN polymer coating on the tubes, that is similar to what is observed in the TEM images. These TEM and AFM observations suggest that the small diameter HiPCO SWNTs may have a stronger interaction with the PAN chains than relatively larger diameter XOC231U FWNTs.

SUMMARY

In summary, for PAN/CNT composite solution prepared under similar processing conditions, CNT bundle sizes in the solution depend on the as-received CNT aspect ratio. The higher the CNT aspect ratio, the more difficult the CNT de-bundling. It was also found that the type of organic solvent affected the CNT bundling behavior, with CNT bundle sizes in DMAc solution larger than those prepared in a DMF solution. Such results indicate better dispersibility of CNTs in DMF than in DMAc. Additionally, the choice of copolymer or homopolymer PAN has negligible effect on the CNT bundle size in the solution. On the other hand, a relatively high concentration of PAN in solution used during the evaporation process reduces bundle size and improves macro-scale homogeneity of the CNTs in the composite solutions. Furthermore, the smaller diameter SWNTs (SPO300) exhibit a stronger interaction with the PAN chains than the relatively larger diameter FWNTs (XOC231U) as observed by TEM and AFM studies.

ACKNOWLEDGMENTS

The authors acknowledge the financial support from DARPA and Army Research Office (grant number W911NF-10-1-0098). The authors also appreciate the help of Dr. Yi-Feng Su at Florida State University for TEM imaging.

REFERENCES

1. Vigolo, B.; Penicaud, A.; Coulon, C.; Sauder, C.; Pailler, R.; Journet, C.; Bernier, P.; Poulin, P. *Science* **2000**, *290*, 1331.
2. Ericson, L. M.; Fan, H.; Peng, H. Q.; Davis, V. A.; Zhou, W.; Sulpizio, J.; Wang, Y. H.; Booker, R.; Vavro, J.; Guthy, C.; Parra-Vasquez, A. N. G.; Kim, M. J.; Ramesh, S.; Saini, R. K.; Kittrell, C.; Lavin, G.; Schmidt, H.; Adams, W. W.; Billups, W. E.; Pasquali, M.; Hwang, W. F.; Hauge, R. H.; Fischer, J. E.; Smalley, R. E. *Science* **2004**, *305*, 1447.
3. Li, Y. L.; Kinloch, I. A.; Windle, A. H. *Science* **2004**, *304*, 276.
4. Behabtu, N.; Young, C. C.; Tsentalovich, D. E.; Kleinerman, O.; Wang, X.; Ma, A. W. K.; Bengio, E. A.; ter Waarbeek, R. F.; de Jong, J. J.; Hoogerwerf, R. E.; Fairchild, S. B.; Ferguson, J. B.; Maruyama, B.; Kono, J.; Talmon, Y.; Cohen, Y.; Otto, M. J.; Pasquali, M. *Science* **2013**, *339*, 182.
5. Liu, Y.; Kumar, S. *ACS Appl. Mater. Interfaces* **2014**, *6*, 6069.
6. Qiu, J. J.; Zhang, C.; Wang, B.; Liang, R. *Nanotechnology* **2007**, *18*, 275708.
7. Moniruzzaman, M.; Winey, K. I. *Macromolecules* **2006**, *39*, 5194.
8. Coleman, J. N.; Khan, U.; Blau, W. J.; Gun'ko, Y. K. *Carbon* **2006**, *44*, 1624.
9. Breuer, O.; Sundararaj, U. *Polym. Compos.* **2004**, *25*, 630.
10. Zhang, X. F.; Liu, T.; Sreekumar, T. V.; Kumar, S.; Moore, V. C.; Hauge, R. H.; Smalley, R. E. *Nano Lett.* **2003**, *3*, 1285.
11. Zhang, X. F.; Sreekumar, T. V.; Liu, T.; Kumar, S. *J. Phys. Chem. B* **2004**, *108*, 16435.
12. Liu, Y.; Kumar, S. *Polym. Rev. (Philadelphia, PA, United States)* **2012**, *52*, 234.
13. Frank, E.; Hermanutz, F.; Buchmeiser, M. R. *Macromol. Mater. Eng.* **2012**, *297*, 493.
14. Huang, X. S. *Materials* **2009**, *2*, 2369.
15. Minus, M. L.; Kumar, S. *JOM* **2005**, *57*, 52.
16. Chae, H. G.; Kumar, S. *Science* **2008**, *319*, 908.
17. Chae, H. G.; Minus, M. L.; Rasheed, A.; Kumar, S. *Polymer* **2007**, *48*, 3781.
18. Chae, H. G.; Choi, Y. H.; Minus, M. L.; Kumar, S. *Compos. Sci. Technol.* **2009**, *69*, 406.
19. Girifalco, L. A.; Hodak, M.; Lee, R. S. *Phys. Rev. B* **2000**, *62*, 13104.
20. Ajayan, P. M.; Tour, J. M. *Nature* **2007**, *447*, 1066.
21. Giordani, S.; Bergin, S.; Nicolosi, V.; Lebedkin, S.; Blau, W. J.; Coleman, J. N. *Phys. Status Solidi B-Basic Solid State Phys.* **2006**, *243*, 3058.
22. Cotiuga, I.; Picchioni, F.; Agarwal, U. S.; Wouters, D.; Loos, J.; Lemstra, P. J. *Macromol. Rapid Commun.* **2006**, *27*, 1073.

23. Islam, M. F.; Rojas, E.; Bergey, D. M.; Johnson, A. T.; Yodh, A. G. *Nano Lett.* **2003**, *3*, 269.

24. Chae, H.; Sreekumar, T.; Uchida, T.; Kumar, S. *Polymer* **2005**, *46*, 10925.

25. Chae, H. G.; Minus, M. L.; Kumar, S. *Polymer* **2006**, *47*, 3494.

26. Liu, T.; Xiao, Z. W. *Macromol. Chem. Phys.* **2012**, *213*, 1697.

27. Liu, T.; Luo, S. D.; Xiao, Z. W.; Zhang, C.; Wang, B. *J. Phys. Chem. C* **2008**, *112*, 19193.

28. Parra-Vasquez, A. N. G.; Stepanek, I.; Davis, V. A.; Moore, V. C.; Haroz, E. H.; Shaver, J.; Hauge, R. H.; Smalley, R. E.; Pasquali, M. *Macromolecules* **2007**, *40*, 4043.

29. Tsentalovich, D. E.; Lee, J. A.; Behabtu, N.; Ma, A. W. K.; Choi, A.; Luo, Y.; Young, C. C.; Pasquali, M. Measuring carbon nanotube aspect ratio with capillary thinning extensional rheology, in preparation.

30. Shaqfeh, E. S. G.; Fredrickson, G. H. *Phys. Fluids A Fluid Dynamics (19891993)* **1990**, *2* 7.

31. Chae, H. G.; Kumar, S. *J. Appl. Polym. Sci.* **2006**, *100*, 791.

32. Xiao, Z.; Gupta, M.; Baltas, G.; Liu, T.; Chae, H. G.; Kumar, S. *Polymer* **2012**, *53*, 5069.

33. Newcomb, B. A.; Chae, H. G.; Gulgunje, P. V.; Gupta, K.; Liu, Y.; Tsentalovich, D. E.; Pasquali, M.; Kumar, S. *Polymer* **2014**, *55*, 2734.